MOLECULAR AND CELLULAR BIOLOGY, Dec. 2004, p. 10448–10455 Vol. 24, No. 23
0270-7306/04/$08.00+0 DOI: 10.1128/MCB.24.23.10448–10455.2004
Copyright © 2004, American Society for Microbiology. All Rights Reserved.

Deficiency in SNM1 Abolishes an Early Mitotic Checkpoint Induced by Spindle Stress†

Shamima Akhter,[1] Christopher T. Richie,[1]‡ Jian Min Deng,[1] Eric Brey,[2] Xiaoshan Zhang,[1] Charles Patrick, Jr.,[2] Richard R. Behringer,[1] and Randy J. Legerski[1]*

Department of Molecular Genetics[1] and Department of Plastic Surgery,[2] The University of Texas M. D. Anderson Cancer Center, Houston, Texas

Received 28 June 2004/Returned for modification 20 July 2004/Accepted 6 September 2004

Spindle poisons represent an important class of anticancer drugs that act by interfering with microtubule polymerization and dynamics and thereby induce mitotic checkpoints and apoptosis. Here we show that mammalian *SNM1* functions in an early mitotic stress checkpoint that is distinct from the well-characterized spindle checkpoint that regulates the metaphase-to-anaphase transition. Specifically, we found that compared to wild-type cells, *Snm1*-deficient mouse embryonic fibroblasts exposed to spindle poisons exhibited elevated levels of micronucleus formation, decreased mitotic delay, a failure to arrest in mitosis prior to chromosome condensation, supernumerary centrosomes, and decreased viability. In addition, we show that both Snm1 and 53BP1, previously shown to interact, coimmunoprecipitate with components of the anaphase-promoting complex (APC)/cyclosome. These findings suggest that Snm1 is a component of a mitotic stress checkpoint that negatively targets the APC prior to chromosome condensation.

SNM1 (sensitivity to nitrogen mustard) is a member of a small gene family that includes four other known mammalian homologs: *Artemis*, *SNM1B*, *CPSF73*, and *ELAC2* (9, 14, 23, 37). The archetypal member of this family, *SNM1*/*PSO2*, was originally identified in *Saccharomyces cerevisiae* as defective in mutants that were highly sensitive to interstrand cross-linking agents such as nitrogen mustard or psoralen plus UVA but not to other forms of DNA damage such as ionizing radiation (IR) or UV radiation (11, 28). The biochemical function of *S. cerevisiae* Snm1 has not been determined, although *snm1* mutants appeared to perform the initial incisions at sites of cross-links normally but were deficient in a later step of restoration of high-molecular-weight DNA from fragmented DNA. This result suggested a defect in the repair of double-strand break (DSB) intermediates that are presumed to occur during cross-link repair (19, 20). All of the *SNM1* family members have in common a region of homology that encodes a metallo-β-lactamase fold (4, 23), while outside of this domain the sequences of the various members are largely divergent. The characterization of the function of the mammalian homologs is largely in the early stages. Gene-targeting methods have been used in mouse embryonic stem (ES) cells to disrupt the *Snm1* gene (9). In contrast to the highly interstrand cross-link sensitive yeast *snm1* mutant, the ES cells in which *Snm1* was disrupted were shown to be only twofold sensitive to mitomycin C and not significantly sensitive to other DNA interstrand cross-linking agents or to IR. Mice homozygous for the disrupted allele were viable and fertile and exhibited no obvious abnormalities; however, treatment of these mice with mitomycin C resulted in increased lethality compared to that of mice heterozygous for the disrupted allele. Nevertheless, these studies appeared to suggest that the function of mammalian *SNM1* differs from that of the yeast gene.

Recently, a novel mitotic stress checkpoint pathway that delays entry into metaphase in the presence of spindle poisons has been identified in mammalian cells (30). This pathway was discovered through characterization of the *Chfr* (checkpoint with FHA and ring finger) gene. In the presence of drugs such as nocodazole or taxol, wild-type cells were found to arrest in prophase, whereas *Chfr*-deficient cells progressed into metaphase. This checkpoint is distinct from the mitotic spindle checkpoint involving Mad and Bub proteins that functions to delay the metaphase-to-anaphase transition in the presence of unattached kinetochores (5, 7, 31, 33).

We show here that *Snm1*-deficient mouse embryonic fibroblasts (MEFs) exhibit a phenotype similar to that of *Chfr*-deficient cells in that upon exposure to spindle poisons, they exhibited elevated levels of mitotic catastrophe, an overall decreased mitotic delay, a failure to arrest prior to chromosome condensation, supernumerary centrosomes, and decreased viability. We also show that both Snm1 and p53 binding protein 1 (53BP1), previously shown to coimmunoprecipitate, interact with the anaphase-promoting complex (APC), a major regulator of mitotic transitions. These findings establish mammalian Snm1 as a checkpoint protein that functions in response to mitotic stress.

* Corresponding author. Mailing address: University of Texas M. D. Anderson Cancer Center, Department of Molecular Genetics, 1515 Holcombe Blvd., Houston, TX 77030. Phone: (713) 792-8941. Fax: (713) 794-4295. E-mail: rlegersk@mdanderson.org.

† Supplemental material for this article may be found at http://mcb.asm.org/.

‡ Present address: National Institute of Diabetes and Digestive and Kidney Diseases, Bethesda, MD 20892.

MATERIALS AND METHODS

Generation of *Snm1* mutant ES cells and mice. A mouse *Snm1* cDNA clone was used to screen a lambda phage mouse (129/SvEv) genomic library to obtain a fragment of the *Snm1* locus. The *Snm1* targeting construct was designed to replace exons 2 to 7 with a *loxP*-flanked PGK*neo*bpA cassette in the opposite transcriptional orientation. Gene targeting in AB1 ES cells and microinjection of targeted clones into C57BL/6J blastocysts were performed as described previously (12). Targeted recombinants were verified by Southern blot analysis using

5′ and 3′ external probes and by PCR analysis. The sequences of PCR primers are as follows: S1, 5′-CATAGAAAATTCCCCTTGGACTATG; S2, 5′-GCCA ATGCATCCGAGGGGCTG; N1, 5′-AGCAAGGGGGAGGATTGGGAAG ACA.

Cell culture. *Snm1*$^{+/+}$ and *Snm1*$^{-/-}$ MEFs were derived from embryos at 13.5 days postconception and grown in Dulbecco's modified Eagle medium with 10% fetal bovine serum, 1× nonessential amino acids, 2-mercaptoethanol (55 mM), penicillin (50 U/ml), and streptomycin (50 U/ml). Cells were cultured according to standard 3T3 protocol and used between passages 3 and 5. Immortalized *Snm1*$^{+/+}$ and *Snm1*$^{-/-}$ cells were obtained at passages 20 and 15, respectively. For synchronization, cells were treated with 2 mM thymidine for 15 h, released into regular medium for 10 h, then treated with 2 mM thymidine for 17 h, and released into 500 ng of nocodazole/ml.

Flow cytometry and analysis of micronuclei. To examine the kinetics of mitotic entry and exit under mitotic stress, lower-passage MEFs were exposed to 125 ng of nocodazole/ml. DNA content, measured by propidium iodide staining, and mitotic index, determined by MPM-2 staining, were analyzed by fluorescence-activated cell sorting (FACS). Formation of micronuclei in the presence of 125 ng of nocodazole/ml, 200 ng of taxol/ml, or 200 ng of Colcemid/ml was determined by 4′,6′-diamidino-2-phenylindole (DAPI) staining and quantitation by fluorescence microscopy. For phenotypic rescue by human SNM1 (hSNM1), cells were transfected with the indicated DNAs and exposed to nocodazole (125 ng/ml) 24 h later. After an additional 24 h of incubation, cells were stained with DAPI and analyzed by fluorescence microscopy.

Time lapse videomicroscopy. MEFs were seeded at 3×10^5 per 25-cm^2 tissue culture flask. Cells in the presence or absence of nocodazole (125 ng/ml) were observed under phase-contrast microscopy on an Olympus (Melville, N.Y.) IX-70 inverted microscope for as long as 24 h. Images were captured every 30 s from numerous locations within the flask by using a color charge-coupled-device camera (C5810; Hamamatsu, Hamamatsu City, Japan). The camera and an XYZ stage were controlled by IPLab image analysis software (Scanalytics, Fairfax, Va.), allowing automated image acquisition at prerecorded locations within the flask. Images were captured by using a 20× air objective (numerical aperture, 0.40) for a pixel resolution of 0.6 μm.

Immunofluorescence. Cells were plated onto glass coverslips, synchronized, and exposed to nocodazole. At the indicated times, coverslips and selectively detached cells (collected by cytospin onto microscope slides) were fixed with 4% paraformaldehyde for 30 min, permeabilized, and blocked with 4% bovine serum albumin and 0.1% Triton X-100 in phosphate-buffered saline for 1 h. Mitotic cells were stained with anti-phosphohistone H3 and fluorescein isothiocyanate-conjugated anti-rabbit immunoglobulin G (IgG) as the secondary antibody. Centrosomes were stained with anti-γ-tubulin and rhodamine-conjugated anti-mouse IgG as the secondary antibody. DNA was stained with DAPI. Prepared slides were analyzed by fluorescence microscopy.

Cdc2 kinase activity and immunoblotting. Cyclin B-associated Cdc2 kinase activity was determined in extracts derived from synchronized cells as described elsewhere (21). Cyclin E and cyclin A levels were determined by immunoblotting as described elsewhere (17). Gel bands were quantified by Kodak 1D Image Analysis software (Eastman Kodak Co., Rochester, N.Y.).

Colony survival assay in response to mitotic stress. Synchronized MEFs were exposed to the indicated concentrations of nocodazole for 8 h. Detached (mitotic) cells were collected and washed twice with phosphate-buffered saline. Subsequently, 200 cells were replated in a 100-mm-diameter dish, and after 2 weeks, colonies were fixed with methanol-acetic acid (3:1) and stained with 4% trypan blue.

Immunoprecipitation. Polyclonal antibodies (designated 3086) to the carboxy-terminal 268 amino acid residues of hSnm1 have been described previously (27). Polyclonal antibodies (designated 6815) to the amino-terminal portion of hSnm1 were raised in rabbits by using amino acid residues 27 to 418 fused to maltose binding protein. Polyclonal antibodies to Cdc27 (H-300) and 53BP1 were obtained from Santa Cruz Biotechnology and generously provided by P. Carpenter, respectively. Coimmunoprecipitation experiments were performed with nuclear or whole-cell extracts essentially as described previously (27).

Inhibition of expression by siRNA. The sequence of the coding strand of the hSNM1 small interfering RNA (siRNA) was CAGAGUGUCCUGAUGGUCU. The efficacy of the hSNM1 siRNA was determined by the following protocol. On day 1, HeLa cells were transfected with a construct expressing enhanced green fluorescent protein (EGFP)-hSNM1. On the following day, the cells were transfected with the hSNM1 or control siRNA and subsequently incubated for another 24 h, after which lysates were prepared for immunoblotting.

RESULTS

Snm1-deficient cells exhibit an aberrant arrest in response to mitotic stress. In a previous report, it was shown that translation of *hSNM1* is controlled by an internal ribosome entry site (IRES) that upregulates its expression during mitosis (40). This finding prompted us to search for a possible mitotic function for this protein. To investigate the role of *Snm1,* we generated mice with a homozygous *Snm1* deletion by targeted disruption in mouse ES cells. The *Snm1*$^{-/-}$ mice were viable and fertile but displayed atypical phenotypes that will be reported on elsewhere. To investigate the possibility of mitotic dysfunction, we exposed asynchronous MEFs to the spindle poison nocodazole for various times and examined them by FACS. This analysis showed that with time of incubation, *Snm1*$^{-/-}$ MEFs displayed a significantly higher increase in the fraction of cells with 4N DNA content than did wild-type cells, indicating an abnormal response to the spindle poison in the absence of functional *SNM1* (Fig. 1a and b). The increase in the fraction of cells with 4N DNA content suggested that *Snm1*$^{-/-}$ cells had failed to undergo normal cytokinesis, whereas wild-type cells were affected to a lesser extent. At higher concentrations of the drug, both cell types failed to undergo normal cytokinesis (data not shown). To assess the possibility of aberrant mitosis, we analyzed both cell types for formation of micronuclei in the presence of nocodazole and two other spindle poisons, Colcemid and taxol, and found that the levels of these aberrant nuclei dramatically increased in *Snm1*$^{-/-}$ cells (Fig. 1c and d). Untreated cells exhibited very low levels of formation of micronuclei. We assayed in total six different *Snm1*$^{-/-}$ MEF isolates from mice derived from two independent ES cell clones, and all exhibited similarly enhanced formation of micronuclei in the presence of spindle poisons. In addition, transfection of a construct expressing *hSNM1* into *Snm1*$^{-/-}$ MEFs resulted in decreased formation of micronuclei in the presence of nocodazole compared to transfection of a vector control (see Fig. S1 in the supplemental material). Furthermore, depletion of *hSNM1* expression in HeLa cells by siRNA resulted in increased formation of micronuclei in the presence of drug (Fig. 1e and f). Taken together, these results indicated that the observed mitotic phenotypes were due to the absence of Snm1.

A mitotic stress checkpoint is defective in Snm1-deficient cells. Micronucleated cells, a signature of mitotic catastrophe, are indicative of a mitotic checkpoint defect, as shown previously in *MAD2*$^{+/-}$ and *Chfr*-deficient cells (21, 30). To assess the possibility of a mitotic checkpoint defect, we synchronized spontaneously immortalized MEFs by a double thymidine block, released them into nocodazole, and monitored the mitotic index by MPM-2 staining and FACS analysis. *Snm1*$^{-/-}$ and wild-type MEFs entered mitosis at the same time after release, but the mutant MEFs exited mitosis approximately 4 to 6 h earlier, suggesting the loss of a mitotic stress-induced checkpoint (Fig. 2a). To confirm altered progression through mitosis, we assayed cyclin B-associated Cdc2 kinase activity in synchronized immortalized MEF cells. Consistent with the results of MPM-2 staining, this assay showed that in the presence of nocodazole, *Snm1*$^{-/-}$ cells lacked the prolonged arrest observed in wild-type cells (Fig. 2b). To quantitate the duration of spindle poison-induced mitotic arrest in asynchronous

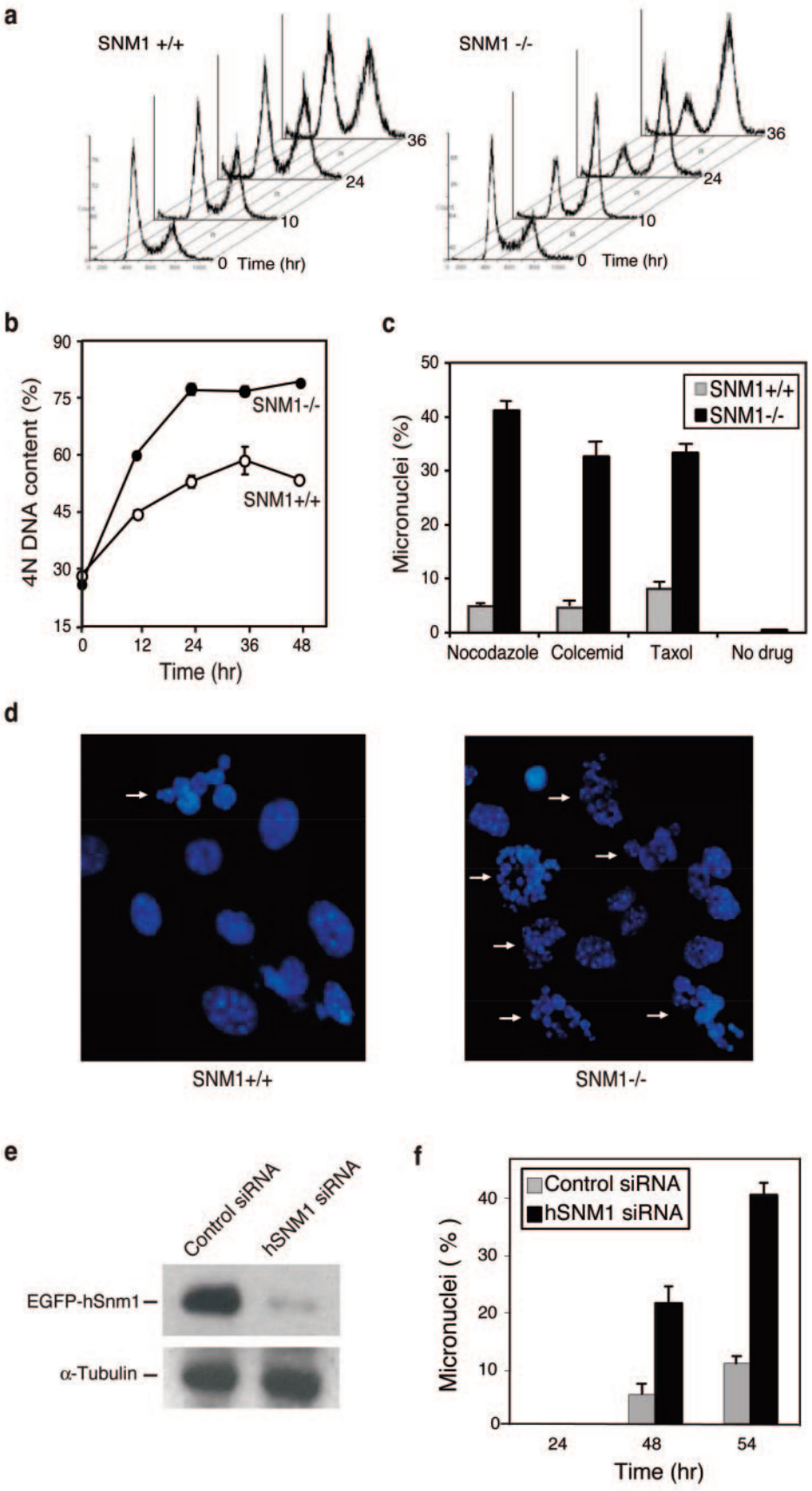
a
SNM1 +/+
SNM1 -/-
36
24
10
0 Time (hr)
b
4N DNA content (%)
SNM1-/-
SNM1+/+
Time (hr)
c
Micronuclei (%)
SNM1+/+
SNM1-/-
Nocodazole
Colcemid
Taxol
No drug
d
SNM1+/+
SNM1-/-
e
Control siRNA
hSNM1 siRNA
EGFP-hSnm1
α-Tubulin
f
Micronuclei (%)
Control siRNA
hSNM1 siRNA
Time (hr)

MEFs, we used live time lapse videomicroscopy. In the absence of nocodazole, the average durations of mitosis were 29.7 ± 4.6 and 36.9 ± 7.9 min in *Snm1*$^{+/+}$ and *Snm1*$^{-/-}$ cells, respectively. When these cells were exposed to nocodazole, the average time in mitosis increased to 9.60 ± 3.00 and 2.73 ± 1.16 h for *Snm1*$^{+/+}$ and *Snm1*$^{-/-}$ cells, respectively (Fig. 2c and d). In addition to the increased duration of mitotic arrest, wild-type cells also exited mitosis more heterogeneously than *Snm1*$^{-/-}$ cells. To confirm that *Snm1*$^{-/-}$ cells exited mitosis more rapidly than wild-type cells in the presence of mitotic stress, we synchronized immortalized MEFs and measured cyclin E levels after release of the MEFs into nocodazole. We observed elevated levels of cyclin E at 16 h after release from the double thymidine block for *Snm1*$^{-/-}$ cells but not until 24 h after release for wild-type cells (Fig. 2e). These results were consistent with the mitotic index data shown in Fig. 2a and also indicated that both cell types ultimately adapted and entered the G_1 phase, although after a longer delay for wild-type cells. In the presence of an active p53-dependent checkpoint pathway, cells with 4N DNA content arrest in G_1 with high cyclin E levels (2, 17). Thus, taken together, these results define a role for *SNM1* in a mitotic stress checkpoint that more than triples the time of cell cycle arrest in the presence of spindle poisons.

The checkpoint defined by Snm1 occurs prior to chromosome condensation. There is increasing evidence that multiple checkpoints regulate the transitions that occur during mitosis. The spindle checkpoint that monitors progression from metaphase to anaphase was originally discovered in budding yeast and has now been well characterized in mammalian cells (7). More recently, a novel checkpoint defined to date by a single factor, Chfr, has been reported to enforce a prophase arrest after exposure of mammalian cells to spindle poisons (30). A pathway monitoring the transition from anaphase to telophase has also been described in yeast (24). To delineate the mitotic checkpoint defined by *SNM1*, we synchronized immortalized MEFs and assessed their mitotic states by monitoring chromosomal condensation and centrosome separation as a function of time after release into nocodazole (Fig. 3a). Quantitation of these states (Fig. 3b) indicated that by 8 h after release, wild-type cells were arrested largely with uncondensed chromosomes, and a high fraction of cells persisted in this stage until at least 16 h. In addition, centrosomes, which normally migrate to opposite poles during prophase, were typically unseparated or in close proximity. In contrast, *Snm1*$^{-/-}$ cells observed at 8 and 12 h were arrested with condensed chromosomes and with widely separated and, in a significant fraction, multiple centrosomes (Fig. 3c). By 16 h, *Snm1*$^{-/-}$ MEFs had progressed through mitosis and a large fraction had formed micronucleated cells. Presumably, the delay observed in *Snm1*$^{-/-}$ MEFs with condensed chromosomes is due to activation of the spindle checkpoint that should be functional in these cells.

To further verify that cell cycle arrest was occurring in mitosis, we examined phosphohistone H3 staining as a function of time after release into nocodazole (Fig. 3d and e). Our results showed that both wild-type and *Snm1*$^{-/-}$ cells had elevated levels of this marker at the time of arrest, indicating that the delay in both cell types occurred during mitosis, consistent with the activation of cyclin B/Cdc2 kinase and the videomicroscopy studies shown above. These experiments also showed that in *Snm1*$^{-/-}$ cells, levels of phosphohistone H3 returned within 16 h to those observed in interphase, while they remained high in wild-type cells, consistent with a reduced mitotic delay in the mutant cells. Taken together, these findings indicate that *SNM1* is involved in a mitotic stress checkpoint that is enforced prior to chromosome condensation. To further define the timing of this checkpoint in mitosis, we examined cyclin A levels in wild-type and mutant cells upon synchronization and release into nocodazole. Cyclin A is degraded during prometaphase in mammalian cells (10) and thus can be used as a marker of early mitosis. As shown in Fig. 3f, cyclin A levels remained high in wild-type cells until about 12 h after release from the thymidine block, whereas in *Snm1*$^{-/-}$ cells, cyclin A levels were greatly reduced by 8 h. These findings confirm a mitotic stress checkpoint defect in *SNM1*-deficient cells and indicate that this checkpoint occurs before the end of prometaphase, indicating that it is distinct from the spindle checkpoint.

To determine if the lack of the early mitotic checkpoint affected viability in the presence of a spindle poison, immortalized MEFs were synchronized and released into nocodazole for 8 h. Mitotic cells were collected, replated into a drug-free medium, and assayed for their ability to form colonies. As shown in Fig. 3g, *Snm1*$^{-/-}$ cells exhibited a dramatic decrease in survival compared to wild-type cells, consistent with a defect in a mitotic stress-induced checkpoint.

Snm1 and 53BP1 interact with the anaphase-promoting complex/cyclosome. The mechanism by which Snm1 enforces a checkpoint response is unknown; however, the APC/cyclosome is a central regulator of mitotic transitions and a primary target of the spindle checkpoint. We therefore examined whether Snm1 and components of the APC physically associate. hSnm1 is a protein expressed at low levels due to the presence of an IRES that depresses translation of the gene (40); nevertheless, as shown in Fig. 4a, antisera raised against two distinct regions of hSnm1 both coimmunoprecipitated the Cdc27 subunit of the APC from HeLa extracts, whereas preimmune sera did not. It has been shown previously that Snm1 and the checkpoint protein 53BP1 interact before and after exposure of cells to IR (27). Thus, as a further verification, we were able to show that antisera to 53BP1 also coimmunoprecipitated Cdc27 (Fig. 4c). Reciprocal immunoprecipitations with anti-Cdc27 antibodies were found to coimmunoprecipitate both hSnm1 and 53BP1, further validating these interactions (Fig. 4b and d). The in-

FIG. 1. Spindle poisons induce mitotic catastrophe in *Snm1*$^{-/-}$ MEFs. (a) FACS profiles of asynchronous wild-type and *Snm1*$^{-/-}$ MEFs exposed to nocodazole (125 ng/ml) for the indicated times and stained with propidium iodide. (b) Graphical presentation of the data shown in panel a. (c) *Snm1*$^{-/-}$ MEFs exposed to the indicated spindle poison for 24 h and analyzed by DAPI staining show increased levels of micronucleated cells. (d) Representative images of cells treated as described for panel c. (e) Immunoblot analysis of depletion of hSnm1 in HeLa cells by siRNA as monitored by the reduction in transiently expressed EGFP-hSnm1. (f) Increased formation of micronuclei in HeLa cells depleted of hSnm1 and exposed to nocodazole (125 ng/ml) for the indicated times.

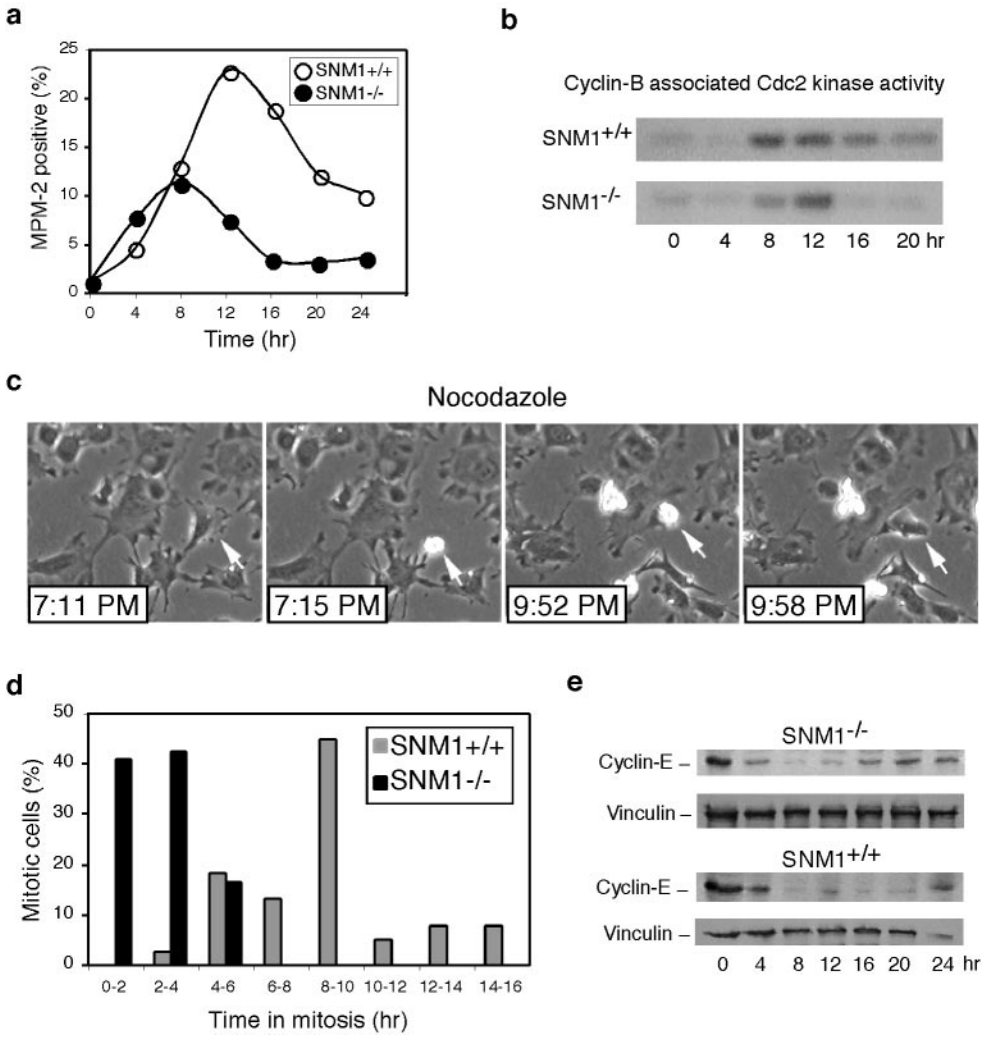

FIG. 2. *Snm1*$^{-/-}$ cells have a mitotic checkpoint defect. (a) FACS profile of synchronized MEFs released from the G_1-S block into nocodazole (0 h) for the indicated times and stained with MPM-2 antibody. (b) Cyclin B-associated Cdc2 kinase activities of synchronized wild-type and *Snm1*$^{-/-}$ MEFs released into nocodazole on a histone H1 substrate. (c) Representative example of determination of mitotic length by videomicroscopy. Arrows in each panel indicate the same cell observed at the indicated times. At least 50 cells were observed for each genotype. (d) Quantitation of time lapse videomicroscopy of wild-type and *Snm1*$^{-/-}$ MEFs at mitosis in the presence or absence of nocodazole. The length of mitosis was determined morphologically by timing when a cell first became rounded and refractile and when it subsequently flattened back onto the surface as shown in panel c. (e) Immunoblot analysis of cyclin E levels in synchronized wild-type and *Snm1*$^{-/-}$ MEFs released into nocodazole from a G_1-S block. Vinculin was used as a loading control.

teraction of 53BP1 with the APC is interesting in light of previous findings showing that 53BP1 is localized to kinetochores and is hyperphosphorylated during mitosis in response to spindle poisons (15). We next examined whether incubation in the presence of nocodazole would enhance the interaction between the APC and either Snm1 or 53BP1. Interestingly, the drug appeared to have little or no effect on the strength of these interactions (Fig. 4e). We therefore examined these interactions as a function of the cell cycle. HeLa cells were fractionated by cell elutriation, and coimmunoprecipitation assays indicated that both Snm1 and 53BP1 constitutively interact with the APC throughout the cell cycle (Fig. 4f). These findings suggest that Snm1 and possibly 53BP1 may act as mediators of an early mitotic checkpoint by targeting the APC.

DISCUSSION

We have demonstrated here that in *SNM1*-deficient cells are defective in a mitotic stress checkpoint that delays entry into metaphase in the presence of spindle poisons. This phenotype is similar to that observed for *Chfr*-deficient cells and suggests that both genes may participate in the same pathway. Analysis of cancer cell lines and primary tumors has shown that *Chfr* is inactivated in a high proportion of these specimens, implying that this pathway is an important mechanism of cancer suppression (30, 32). In addition, inactivation of this pathway may also explain why some tumors are highly susceptible to the cytotoxic activity of spindle poisons. In the original report on the role of Chfr in a mitotic stress checkpoint, it was concluded

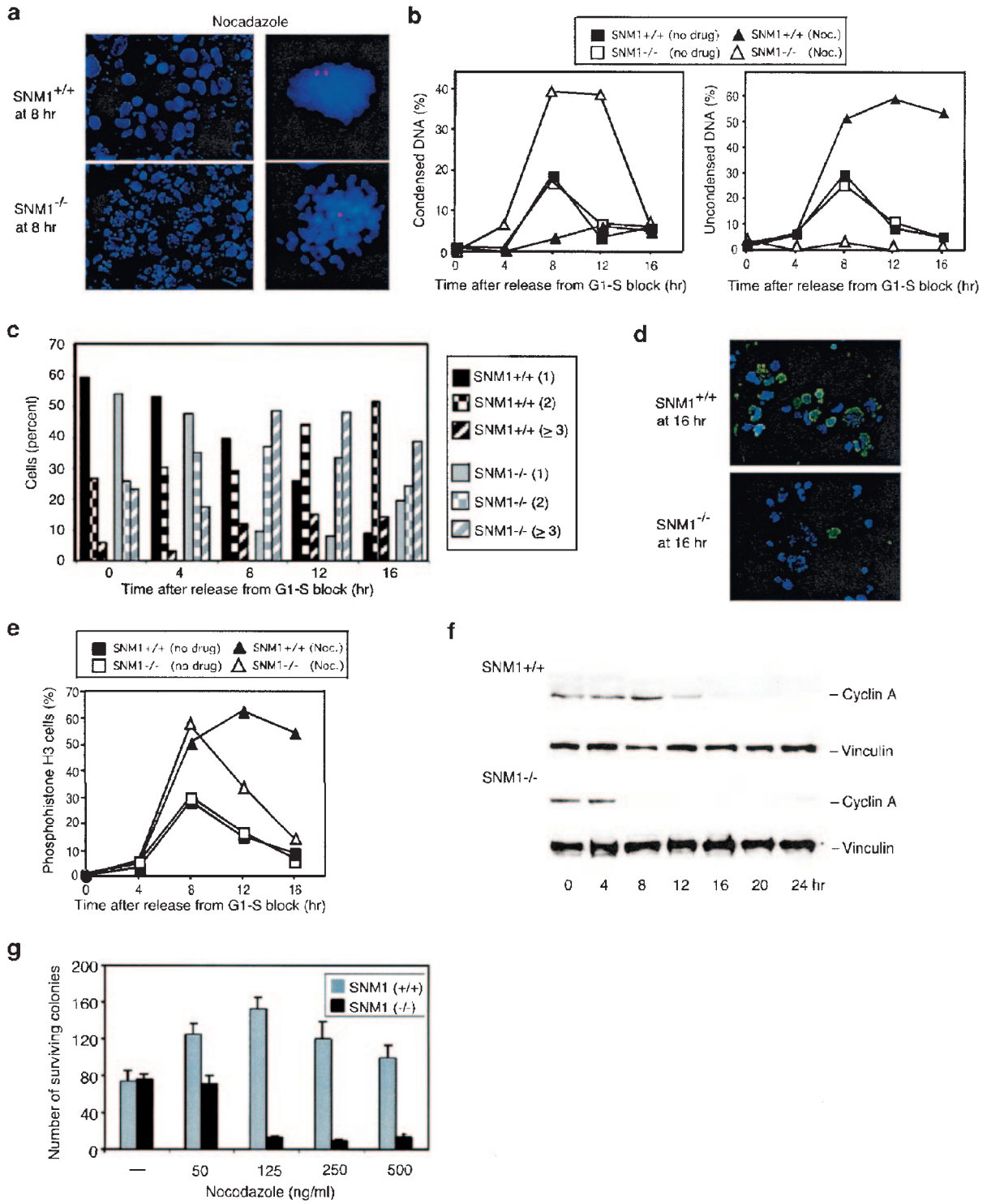

FIG. 3. SNM1 defines an early mitotic checkpoint. (a) Representative images of wild-type and *Snm1*$^{-/-}$ MEFs synchronized, released into nocodazole, and analyzed by DAPI staining. In the right panels, centrosomes (red) were identified by indirect immunofluorescence of γ-tubulin. (b) Fractions of cells with condensed DNA and widely separated centrosomes (left panel) and of cells with uncondensed DNA and slightly separated centrosomes (right panel) as a function of time after release from a G_1-S block. Noc., nocodazole. (c) Quantitation of centrosome number after release into nocodazole. In the key, the numbers of centrosomes observed are given in parentheses. (d) Representative images of wild-type and *Snm1*$^{-/-}$ MEFs synchronized, released into nocodazole, and analyzed for phosphohistone H3 staining (green). DNA was stained with DAPI (blue). (e) Fraction of phosphohistone H3-positive cells as a function of time after release into nocodazole from a G_1-S block. (f) Immunoblot analysis of cyclin A levels in synchronized wild-type and *Snm1*$^{-/-}$ MEFs released into nocodazole from a G_1-S block. (g) Colony survival assay of wild-type and *Snm1*$^{-/-}$ MEFs exposed to nocodazole at the indicated concentrations.

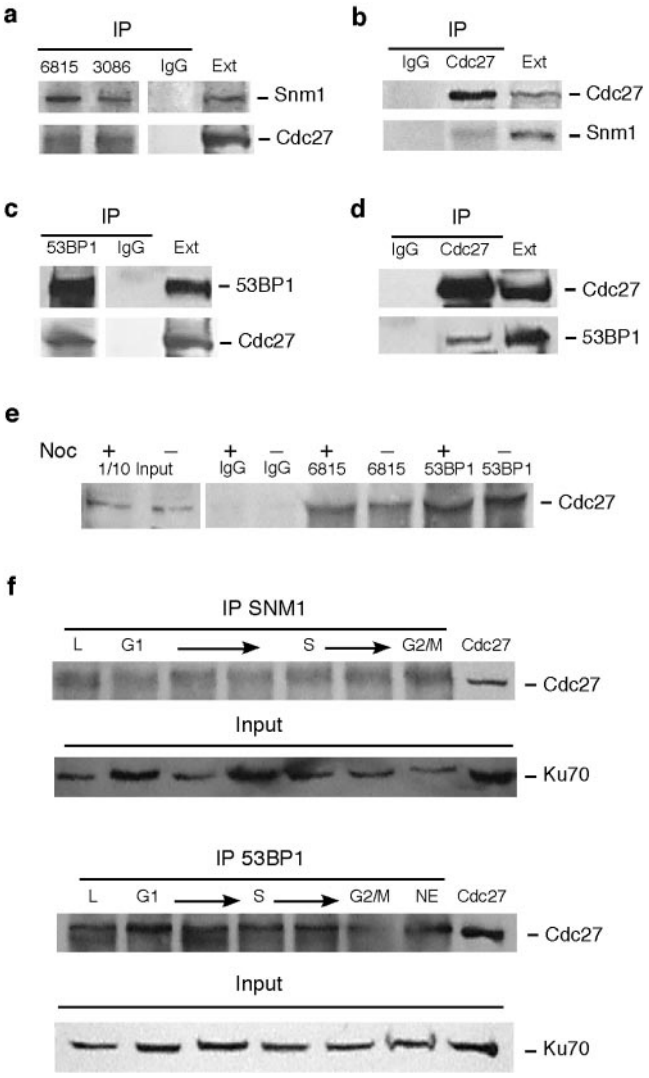

FIG. 4. Snm1 and 53BP1 coimmunoprecipitate with the Cdc27 component of the APC. (a and b) Reciprocal coimmunoprecipitations (IP) of Snm1 and Cdc27 and analysis by immunoblotting. Antibodies 6815 and 3086 were raised against the amino-terminal and carboxy-terminal regions of hSnm1, respectively. "IgG" indicates control immunoprecipitations with preimmune serum. "Ext" indicates loading of untreated whole-cell extracts from HeLa cells. (c and d) Reciprocal coimmunoprecipitations of 53BP1 and Cdc27. (e) Incubation of cells with nocodazole (Noc) for 24 h does not enhance the interaction between the APC and either Snm1 or 53BP1 as determined by coimmunoprecipitation. (f) Snm1 and 53BP1 constitutively interact with the APC throughout the cell cycle. HeLa cells were fractionated as a function of the cell cycle by elutriation.

that the delay in the presence of spindle poisons was enforced during prophase. However, subsequent studies with *Xenopus* extracts showed that Chfr is a ubiquitin ligase that targets Polo-like kinase 1 (Plk1) for destruction by the proteasome (16). Degradation of Plk1 was proposed to result in a delay in the activation of the Cdc25C phosphatase and the inactivation of the Wee1 kinase, ultimately causing a delay in the activation of Cdc2–cyclin B. In this proposed pathway, the checkpoint would prevent the G_2-to-M transition (22). However, our findings and those reported by others (30) showed that Cdc2–cyclin B is activated in the presence of spindle poisons in mammalian cells. In addition, our studies by videomicroscopy and on the phosphorylation of histone H3 indicate that the checkpoint is enforced during mitosis. Moreover, a study with HeLa cells has shown that activation of Cdc2–cyclin B is independent of Plk1 with or without exposure of cells to nocodazole (18). Thus, these results indicate that Cdc2–cyclin B is not the target of the checkpoint and that the checkpoint is enforced after activation of this kinase during prophase but before its degradation in metaphase (6). Additionally, our examination of cyclin A levels indicated that the checkpoint occurs prior to the degradation of this protein, which occurs during prometaphase (10). Interestingly, a recent analysis of the tumor suppressor RASSF1A showed that it is a negative regulator of the APC and that its overexpression in mammalian cells causes early mitotic arrest due to a failure to degrade cyclin A (34). This finding thus established the principle that inhibition of the APC can result in an early mitotic arrest that occurs prior to and is independent of the spindle checkpoint pathway that operates in metaphase. Therefore, as a working model, we propose that Snm1 acts in a mitotic stress checkpoint pathway that negatively targets the APC, resulting in arrest in early mitosis prior to chromosome condensation.

Prior studies of Snm1 in human cells have shown that it is a nuclear protein that forms foci at sites of DNA DSBs induced by IR (27). These foci colocalize with those containing γ-H2AX, 53BP1, and components of the BRCA1-associated surveillance complex (1, 25, 26, 29, 38, 39). In fact, both Snm1 and γ-H2AX coimmunoprecipitate with 53BP1, suggesting that all three of these proteins reside in a common complex (1, 27). These findings may appear at odds with the results described above showing the involvement of Snm1 in a mitotic stress checkpoint; however, it has been demonstrated that the spindle poison paclitaxel causes DNA strand breaks in proliferating human cells by an indirect mechanism (3, 8). Thus, conceivably the stimulus for the early mitotic checkpoint may be DNA damage as opposed to microtubule disruption per se, a hypothesis that is more consistent with the demonstrated localization of Snm1 and 53BP1 to sites of DSBs during the interphase of the cell cycle. The timing of the checkpoint, prior to chromosome condensation, might facilitate DNA repair processing, which would be problematic on condensed chromatin. Further support for this model comes from the finding that the APC has been shown to be a target of a DNA damage checkpoint in chicken cells (35). In addition, recent studies have shown that DNA damage during mitosis is a trigger for a response that results in centrosome inactivation and fragmentation and that prevents the proliferation of cells with genomic instability (13, 36). In many respects these findings are consistent with our own results, which suggest that Snm1 may participate in a pathway that monitors genome integrity during mitosis in order to prevent aberrant chromosomal segregation and ultimately tumorigenesis. Alternatively, Snm1 may participate in multiple checkpoint pathways that respond to various types of cellular stress.

ACKNOWLEDGMENTS

We thank J. Schumacher and L. Li for comments and advice.

This work was supported by NCI grants CA52461, CA90270, and CA96574 and EHS grant ES07784. DNA sequencing and veterinary

resources were supported by Cancer Center Support (Core) grant CA16672.

REFERENCES

1. **Anderson, L., C. Henderson, and Y. Adachi.** 2001. Phosphorylation and rapid relocalization of 53BP1 to nuclear foci upon DNA damage. Mol. Cell. Biol. **21:**1719–1729.
2. **Andreassen, P. R., O. D. Lohez, F. B. Lacroix, and R. L. Margolis.** 2001. Tetraploid state induces p53-dependent arrest of nontransformed mammalian cells in G_1. Mol. Biol. Cell **12:**1315–1328.
3. **Bleicher, R. J., H. Xia, H. A. Zaren, and S. V. Singh.** 2000. Biochemical mechanism of cross resistance to paclitaxel in a mitomycin C-resistant human bladder cancer cell line. Cancer Lett. **150:**129–135.
4. **Callebaut, I., D. Moshous, J. P. Mornon, and J. P. de Villartay.** 2002. Metallo-β-lactamase fold within nucleic acids processing enzymes: the β-CASP family. Nucleic Acids Res. **30:**3592–3601.
5. **Cerutti, L., and V. Simanis.** 2000. Controlling the end of the cell cycle. Curr. Opin. Genet. Dev. **9:**65–69.
6. **Chang, D. C., N. Xu, and K. Q. Luo.** 2003. Degradation of cyclin B is required for the onset of anaphase in mammalian cells. J. Biol. Chem. **278:**37865–37873.
7. **Cleveland, D. W., Y. Mao, and K. F. Sullivan.** 2003. Centromeres and kinetochores: from epigenetics to mitotic checkpoint signaling. Cell **112:**407–421.
8. **Digue, L., T. Orsiere, M. De Meo, M. G. Mattei, D. Depetris, F. Duffaud, R. Favre, and A. Botta.** 1999. Evaluation of the genotoxic activity of paclitaxel by the in vitro micronucleus test in combination with fluorescent in situ hybridization of a DNA centromeric probe and the alkaline single cell gel electrophoresis technique (comet assay) in human T-lymphocytes. Environ. Mol. Mutagen. **34:**269–278.
9. **Dronkert, M. L., J. de Wit, M. Boeve, M. L. Vasconcelos, H. T. van Steeg, L. Tan, J. H. Hoeijmakers, and R. Kanaar.** 2000. Disruption of mouse SNM1 causes increased sensitivity to the DNA interstrand cross-linking agent mitomycin C. Mol. Cell. Biol. **20:**4553–4561.
10. **Geley, S., E. Kramer, C. Gieffers, J. Gannon, J.-M. Peters, and T. Hunt.** 2001. Anaphase-promoting complex/cyclosome-dependent proteolysis of human cyclin A starts at the beginning of mitosis and is not subject to the spindle assembly checkpoint. J. Cell Biol. **153:**137–147.
11. **Henriques, J. A., and E. Moustacchi.** 1980. Isolation and characterization of *pso* mutants sensitive to photoaddition of psoralen derivatives in *Saccharomyces cerevisiae*. Genetics **95:**273–288.
12. **Horan, G. S., E. N. Kovacs, R. R. Behringer, and M. S. Featherstone.** 1995. Mutations in paralogous Hox genes result in overlapping homeotic transformations of the axial skeleton: evidence for unique and redundant function. Dev. Biol. **169:**359–372.
13. **Hut, H. M. J., W. Lemstra, E. H. Blaauw, G. W. A. van Cappellen, H. H. Kampinga, and O. C. M. Sibon.** 2003. Centrosomes split in the presence of impaired DNA integrity during mitosis. Mol. Biol. Cell **14:**1993–2004.
14. **Jenny, A., L. Minvielle-Sebastia, P. J. Preker, and W. Keller.** 1996. Sequence similarity between the 73-kilodalton protein of mammalian CPSF and a subunit of yeast polyadenylation factor I. Science **274:**5292–5293.
15. **Jullien, D., P. Vagnarelli, W. C. Earnshaw, and Y. Adachi.** 2002. Kinetochore localisation of the DNA damage response component 53BP1 during mitosis. J. Cell Sci. **115:**71–79.
16. **Kang, D., J. Chen, J. Wong, and G. Fang.** 2002. The checkpoint protein Chfr is a ligase that ubiquitinates Plk1 and inhibits Cdc2 at the G_2 to M transition. J. Cell Biol. **156:**249–259.
17. **Lanni, J. S., and T. Jacks.** 1998. Characterization of the p53-dependent postmitotic checkpoint following spindle disruption. Mol. Cell. Biol. **18:**1055–1064.
18. **Liu, X., and R. L. Erikson.** 2002. Activation of Cdc2/cyclin B and inhibition of centrosome amplification in cells depleted of Plk1 by siRNA. Proc. Natl. Acad. Sci. USA **99:**8672–8676.
19. **Magana-Schwencke, N., J. A. Henriques, R. Chanet, and E. Moustacchi.** 1982. The fate of 8-methoxypsoralen photoinduced crosslinks in nuclear and mitochondrial yeast DNA: comparison of wild-type and repair-deficient strains. Proc. Natl. Acad. Sci. USA **79:**1722–1726.
20. **Meniel, V., N. Magana-Schwencke, and D. Averbeck.** 1995. Preferential repair in *Saccharomyces cerevisiae rad* mutants after induction of interstrand cross-links by 8-methoxypsoralen plus UVA. Mutagenesis **10:**543–548.
21. **Michel, L. S., V. Liberal, A. Chatterjee, R. Kirchwegger, B. Pasche, W. Gerald, M. Dobles, P. K. Sorger, and R. Benezra.** 2001. MAD2 haploinsufficiency causes premature anaphase and chromosome instability in mammalian cells. Nature **409:**355–359.
22. **Mikhailov, A., and C. L. Rieder.** 2002. Cell cycle: stressed out of mitosis. Curr. Biol. **12:**R331–R333.
23. **Moshous, D., I. Callebaut, R. de Chasseval, B. Corneo, M. Cavazzana-Calvo, F. Le Deist, I. Tezcan, O. Sanal, Y. Bertrand, N. Phillippe, A. Fischer, and J. P. de Villartay.** 2001. Artemis, a novel DNA double-strand break repair/V(D)J recombination protein, is mutated in human severe combined immune deficiency. Cell **105:**177–186.
24. **Muhua, L., N. R. Adames, M. D. Murphy, C. R. Shields, and J. A. Cooper.** 1998. A cytokinesis checkpoint requiring the yeast homologue of an APC-binding protein. Nature **393:**487–491.
25. **Paull, T. T., E. P. Rogakou, V. Yamazaki, C. U. Kirchgessner, M. Gellert, and W. M. Bonner.** 2000. A critical role for histone H2AX in recruitment of repair factors to nuclear foci after DNA damage. Curr. Biol. **10:**886–895.
26. **Rappold, I., K. Iwabuchi, T. Date, and J. Chen.** 2001. Tumor suppressor p53 binding protein 1 (53BP1) is involved in DNA damage-signaling pathways. J. Cell Biol. **153:**613–620.
27. **Richie, C. T., C. A. Peterson, T. Lu, W. N. Hittelman, P. B. Carpenter, and R. J. Legerski.** 2002. hSnm1 colocalizes and physically associates with 53BP1 before and after DNA damage. Mol. Cell. Biol. **22:**8635–8647.
28. **Ruhland, A., M. Kircher, F. Wilborn, and M. Brendel.** 1981. A yeast mutant specifically sensitive to bifunctional alkylation. Mutat. Res. **91:**457–462.
29. **Schultz, L. B., N. H. Chehab, A. Malikzay, and T. D. Halazonetis.** 2000. p53 binding protein 1 (53BP1) is an early participant in the cellular response to DNA double-strand breaks. J. Cell Biol. **151:**1381–1390.
30. **Scolnick, D. M., and T. D. Halazonetis.** 2000. Chfr defines a mitotic stress checkpoint that delays entry into metaphase. Nature **406:**430–435.
31. **Shah, J. V., and D. W. Cleveland.** 2000. Waiting for anaphase: Mad2 and the spindle assembly checkpoint. Cell **103:**997–1000.
32. **Shibata, Y., N. Haruki, Y. Kuwabara, H. Ishiguro, N. Shinoda, A. Sato, M. Kimura, H. Koyama, T. Toyama, T. Nishiwaki, J. Kudo, Y. Terashita, S. Konishi, H. Sugiura, and Y. Fujii.** 2002. Chfr expression is downregulated by CpG island hypermethylation in esophageal cancer. Carcinogenesis **23:**1695–1699.
33. **Smith, P. L., J. F. Gimenez-Abian, and D. J. Clarke.** 2002. DNA-damage-independent checkpoints: yeast and higher eukaryotes. Cell Cycle **1:**16–33.
34. **Song, M. S., S. J. Song, N. G. Ayad, J. S. Chang, J. H. Lee, H. K. Hong, H. Lee, N. Choi, J. Kim, H. Kim, J. W. Kim, E.-J. Choi, M. W. Kirschner, and D.-S. Lim.** 2004. The tumour suppressor RASSF1A regulates mitosis by inhibiting the APC–Cdc20 complex. Nat. Cell Biol. **6:**129–137.
35. **Sudo, T., Y. Ota, S. Kotani, M. Nakao, Y. Takami, S. Takeda, and H. Saya.** 2001. Activation of Cdh1-dependent APC is required for G_1 cell cycle arrest and DNA damage-induced G_2 checkpoint in vertebrate cells. EMBO J. **20:**6499–6508.
36. **Takada, S., A. Kelkar, and W. E. Theurkauf.** 2003. *Drosophila* checkpoint kinase 2 couples centrosome function and spindle assembly to genomic integrity. Cell **113:**87–99.
37. **Tavtigian, S. V., J. Simard, D. H. Teng, V. Abtin, M. Baumgard, A. Beck, N. J. Camp, A. R. Carillo, Y. Chen, P. Dayananth, M. Desrochers, M. Dumont, J. M. Farnham, D. Frank, C. Frye, S. Ghaffari, J. S. Gupte, R. Hu, D. Iliev, T. Janecki, N. Kort, K. E. Laity, A. Leavitt, G. Leblanc, G. McArthur-Morrison, A. Pederson, B. Penn, K. T. Peterson, J. E. Reid, S. Richards, M. Schroeder, R. Smith, S. C. Snyder, B. Swedlund, B. Swensen, A. Thomas, M. Tranchant, A. M. Woodland, F. Labrie, M. H. Skolnick, S. Neuhausen, J. Rommens, and L. A. Cannon-Albright.** 2001. A candidate prostate cancer susceptibility gene at chromosome 17p. Nat. Genet. **27:**172–180.
38. **Wang, Y., D. Cortez, P. Yazdi, N. Neff, S. J. Elledge, and J. Qin.** 2000. BASC, a super complex of BRCA1-associated proteins involved in the recognition and repair of aberrant DNA structures. Genes Dev. **14:**927–939.
39. **Xia, Z., J. C. Morales, W. G. Dunphy, and P. B. Carpenter.** 2001. Negative cell cycle regulation and DNA damage-inducible phosphorylation of the BRCT protein 53BP1. J. Biol. Chem. **276:**2708–2718.
40. **Zhang, X., C. T. Richie, and R. J. Legerski.** 2002. Translation of hSNM1is mediated by an internal ribosome entry site that upregulates expression during mitosis. DNA Repair **1:**379–390.